Article

Equilibrium and Kinetic study of lead and copper ions adsorption on Chitosan-grafted-poly acrylic acid synthesized by Surface initiated Atomic Transfer Polymerization

Carlos Grande [1], William Vallejo [2,*] and Fabio Zuluaga [3]

[1] Grupo de Fotoquímica y fotobiología, Universidad del Atlántico; carlosgrande@mail.uniatlantico.edu.co

[2] Grupo de Fotoquímica y fotobiología, Universidad del Atlántico; williamvallejo@mail.uniatlantico.edu.co

[3] Departamento de Química, Universidad del Valle hector.zuluaga@correounivalle.edu.co

* Correspondence: williamvallejo@mail.uniatlantico.edu.co; Tel.: +5753599484

Abstract: In this work, we synthesized chitosan grafted-poly acrylic acid (CS-g-PA) through surface-initiated atom transfer radical polymerization (SI-ATRP). We also studied the adsorption process of copper and lead ions onto CS-g-PA surface. Adsorption equilibrium studies indicated pH 4.0 as the best pH for the adsorption process, while the maximum adsorption capacity for Pb^{2+} ions was 98 $mg*g^{-1}$ and for Cu^{2+} was 164 $mg*g^{-1}$, higher adsorption capacities than chitosan alone (CS), where Pb^{2+} was only 14.8 $mg*g^{-1}$ and Cu2+ was 140 $mg*g^{-1}$, respectively. Furthermore, the adsorption studies indicated that Langmuir model describes all the experimental data. All these results suggest that the new CS-g-PA polymers had potential as adsorbent for hazardous and toxic metal ions produced by different industries.

Keywords: ATRP, chitosan grafted poly acrylic acid, heavy metals; adsorption; water treatment.

1. Introduction

The presence in the water of metals dangerous to health generated by industrial activities, such as lead and copper, have led to the search for removal efficient methods that do not generate problems of subsequent contamination; currently, lead and copper are reported between the most toxic metals to the environment [1]. From lasts decade, they have drawn much attention owing to its impact on the public health and toxicity; the Environmental Protection Agency of the United States, EPA has classified some heavy metal ions as priority pollutants due to its high degree of toxicity and hazardous when they are presented in water and recently have published "Use of Lead Free Pipes, Fittings, Fixtures, Solder and Flux for Drinking Water; Extension of Comment Period" [2]. The main sources for lead and cupper are wastewater discharge, mining activities, phosphate fertilizers, industries textile, leather, plumbing manufacturing, electric wires, pigments, electroplating, municipal waste, sewage waste, welding, galvanized steel, between others [3]. Lead, for example, represents a serious hazardous because of a cumulative effect and ability to damage central nervous system. This metal is commonly found in minerals such as *galena* and *cerussite* for the manufacturing of batteries, welding, paints, pyrotechnics, pottery, glassware and mining; according to the WHO, the maximum levels of lead in blood must be 0.05 mg/L [4]. Copper is a metal used in electrical, electronics and metal materials, due to its high electrical conductivity, ductility and malleability. In turn, it is also necessary in some biological processes (i.e., myelin formation of hemoglobin and excessive blood clotting prevention acting as a coenzyme of the immune system and regulating the production of melanin [5]. However, high concentrations of this element in body affect health, causing headaches, nausea, vomiting, diarrhea, liver, blood, vessels and kidney damage; furthermore, exposure to copper for a long time can irritates the nose, mouth, eyes and respiratory system; permissive level given by the WHO for Cu (II) into drinking water is 0.05 g/mL [6,7]. Different

approaches have been employed to solve the growing need of lead and cupper ions removal from water including chemical precipitation, membrane separation, ion exchange, coagulation and adsorption [7,8]. Among all these technologies, adsorption is the most promising methodology. Generally, materials that are able to remove lead and cupper ions carry nitrogen, oxygen and sulfur functional groups as the binding sites. Therefore, natural adsorbents, agricultural waste and biopolymers have attracted considerable attention due to their low cost and abundance in nature and high efficiency, to remove heavy metal ions from waste water [9]. Chitosan is a biopolymer of high interest because of its biocompatibility and antimicrobial effect against different microorganism, that comes from the partial deacetylation of chitin, a polysaccharide obtained from the exoskeleton of crustaceans and the mycelium of some fungi [10]. Chitosan can form films and poses chelating properties, reason why it has been used in different preparations (beads, nanobeads, nanoparticles, etc.) to remove heavy metal   from different source [11]. Chitosan beads, for example, have been used effectively to remove lead and cupper [12]. Different reports have suggested that the mechanism for lead and cupper complexation by chitosan/PVA and chitosan/cellulose hydrogels could be the result of a combination of chemical complexation, ion-exchange and non-specific electrostatic interaction, depending on the solution pH [13]. Surface-initiated polymerization has emerged as one of the most important techniques to modify surface properties of materials, with important effects on the fields of optoelectronics, biosciences and engineering [14]. Surface-initiated atomic radical polymerization, SI-ATRP, is a versatile method for the preparation of different hybrid materials, with a particular control over molecular weight and poly dispersities, allowing control over molecular architectures[15]. SI-ATRP does not require stringent experimental conditions like other ionic living polymerization techniques having a high versatility for the polymerization of different monomers. Poly methacrylic acid brushes, for example, have been prepared by SI-ATRP using a two steps procedure with protective groups to avoid catalyst poisoning [16,17]. However, the use of protecting groups in some cases could be expensive and tiring process. Water treatment with surface modified adsorbents such as poly acrylic acid could be interesting, improvement of the adsorption properties, resulting from the insolubility, higher adsorption capacities and easiness of the purification process (a simple filtration at the end) to remove pollutants. Chitosan-grafted with polymers by different methodologies and materials have been used to remove lead and cupper with promising achievements [9,18,19].

In this work, we report the surface modification of chitosan by surface initiated ATRP with poly (sodium acrylate), in order to increase their ability to remove heavy metals such as lead and copper.

2. Materials and Methods

2.1. Materials

Chemical reagents were purchased from Aldrich and used without further purification unless otherwise stated. Chitosan was purchased from KOYO Chemical Co. (M_w = 233 KDa, M_n = 105 KDa, PDI = 2.2, determined by GPC). Silicon substrates (silica wafers: SiO_2 layers of 200 nm, doped with boron; face 100, p-type) were purchased from World KST Co. (Fukui, Japan), and were cut in the size convenient (typically 4 cm²) immersed in a mixture of sulfuric acid and hydrogen peroxide [piranha solution (3:1)] for a 10-minute washing and then washed with deionized water (18.2 milliohms cm). 2-bromo isobutyryl bromide (2-BIB, 97%) was obtained from ALFA AESAR, USA. CuBr, $CuBr_2$, N,N,N',N'',N''-pentamethyldiethylenetriamine (PMDETA), and triethylamine (99.5%) were purchased from Sigma-Aldrich and used as received. The standard solutions of Lead (II) and copper (II) of 1000 mg/L were purchased from Merck. Other chemicals were purchased from Sigma-Aldrich and used as they were received.

2.2. Synthesis

The ATRP initiator was grafted on the surface of chitosan (figure 1) using a modified reported procedure [20]: 5g of chitosan (Deacetylation degree of 85%, medium molecular weight, Sigma-Aldrich, Palo Alto, California) were added to a schlenk tube containing a solution of 25mL of dry

THF (Sigma-Aldrich, Palo Alto, California) and 0.5mL of triethylamine (99%, Aldrich, Palo Alto, California). The tube was immersed in an ice bath and sealed using a septum. The content was gently stirred using a magnetic bar and purged with N_2 during 30 min after what, 0.5mL of 2-bromopropionyl bromide (2-BIB) (Sigma-Aldrich, Milwaukee, USA) was added under nitrogen dropwise placed in an ice bath. The reaction was removed from the ice bath and allowed to warm to room temperature and react overnight. Chitosan grafted BIB (CS-*g*-BIB) was filtered and washed extensively with THF, methanol and deionized water, DI, and allowed to dry in a vacuum oven at 40°C for 48 hours. 0.5g of CS-*g*-BIB was carefully added to another schlenk tube with 21.51mg (150 μmol) of CuBr (Sigma-Aldrich, Palo Alto, California) and 3.35 mg (15 μmol) of $CuBr_2$ (Sigma-Aldrich, Palo Alto, California), sealed with a septum and flushed with N_2 for 40 minutes. In a second Schlenk tube, 1.0g (10.63 mmol) of sodium acrylate (Sigma-Aldrich, Milwaukee, USA) was added to a mixture of 111L (0.530 mmol) of N,N,N',N'',N''-pentamethyldiethylenetriamine (PMDETA), and 17.5mL of DI water/methanol (1:1). The contents were gently stirred and degassed with nitrogen for 40 minutes and transferred using cannula to the first tube. The polymerization proceeded for 24 hours. CS-*g*-PA was washed with DI water in an ultrasonic bath, centrifuged and dried after water discard. The resultant chitosan was washed with large amounts of deionized water and followed was immersed in an acidic solution (0.1M HCl) to remove any physically adsorbed reactant and to protonate the acrylic acid groups (ion exchange between Na^+ to H^+). Finally, the CS-g-PA obtained was dried in a vacuum oven at 40°C for 48 hours and stored in a desiccator for subsequent use [21].
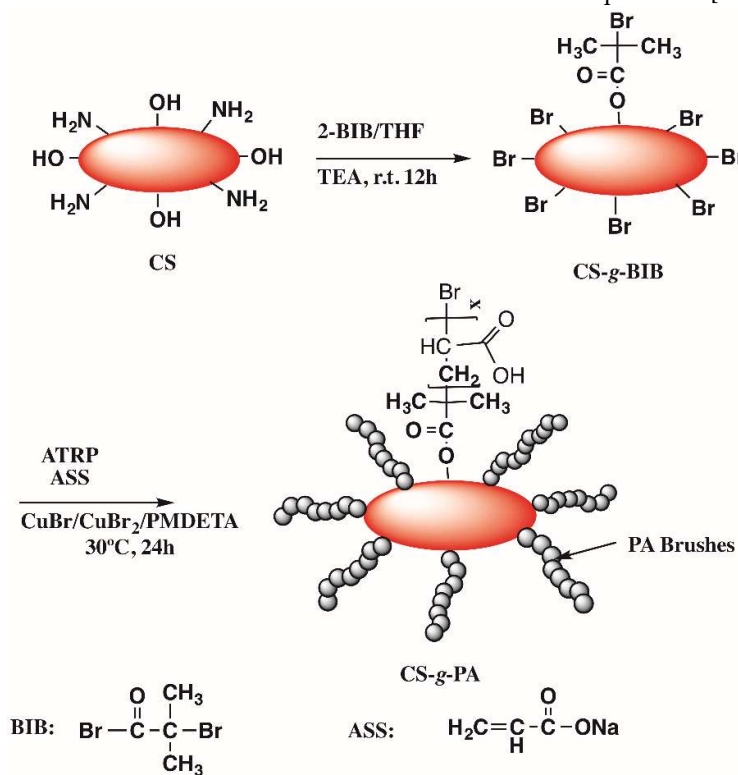

Figure 1. Schematic diagram for the synthesis of chitosan grafted poly acrylate from chitosan.

2.3. Adsorption Assay

The pH study effect on adsorption experiments were carried out by using 25 mg of the adsorbent (CS or CS-*g*-PA) in 50 mL of the initial metal solution at different pH (between 1 and 7) using an initial concentration of the metal of 200 ppm for 24 hours at 25°C under stirring. After pH study, the adsorption experiments were carried out by using 25 mg of the adsorbent in 50 mL of the initial metal

solution of metal solution concentration of 100, 200, 300, 400 and 500 ppm for 24 hours at 25°C, at pH 4.0 under stirring. Metal concentration was determined by atomic absorption spectrophotometry for using calibration curves; Atomic absorption measurements were performed on a Perkin Elmer 200 Analyst using the flame method to determining the concentration of metal ion remaining in solution. NIST Lead and Cupper standards were used to prepare calibration curves, with 1000 mg/L as stock solution and dilutions with concentrations of 1.0037, 1.9975, 3.0012, 3.995 and 4.9987 ppm, for cupper and 1.000, 2.000, 3.000 4.000 and 5.000 ppm for lead, with hollow cathode lamps at 324 nm for cupper and 217 nm for lead determination. Finally, the studies of metal adsorption kinetics were carried out using at pH 4.0 for using 200 ppm as the initial concentration of the metal ion at temperature of 25°C and 25 mg of adsorbent under stirring.

3. Discussion

3.1. Shyntesis

Direct ATRP polymerization of acid monomers can be affected by the reaction of the monomer with metal ions to form complexes that are catalytically ineffective [17]. Several authors have synthesized polymer brushes such as poly methacrylic acid and poly acrylic acid using tert-butyl acrylate and tert-butyl methacrylate via ATRP, using pyrolysis or hydrolysis of the protecting group tert-butyl ester [22]. However, this methodology introduces additional steps and produces loss of some polymer chains from the surface [17]. It is clear that direct insertion of the acidic polymer chains is a challenge by ATRP. One possibility is to use a previously reported procedure that uses sodium salts of the acids and later acidification [17,23]. The SI-ATRP modification of chitosan particles was previously published by our group [21], but it is shortly discussed here. As we published earlier, the polymerization reaction of sodium acrylate was first conducted on silicon wafer surfaces modified by spin coated chitosan. The polymerization conditions were: 100:2:0.4:5:1400 for NaAA: CuBr: CuBr2: PMDETA in a mixture of water : methanol 1:1. However, with an increasing of the molar ratio to 300:2:0.4:1400 for NaAA: CuBr:CuBr2:PMDETA and a decreasing in the temperature of the system from 60ºC to 25ºC, the thickness of the system is increased as a result of a decreasing of the hydrolysis chain from the silicon surfaces. Details of characterization are reported in previous work by Grande [21].

3.2. pH effect on Adsorption process

The number of ions adsorbed on adsorbent's surface is normally described by the mass balance equation: $q_{t_i} = \frac{\sum_{i=1}^{n}(c_{t_{i-1}} - c_{t_i})v_{t_{i-1}}}{m}$ (2), where C_{ti-1} is the initial concentration of the ion, C_{ti} is the concentration of the ion at time *t*, V_{ti-1} is the initial volume of the solution and m is the mass of the adsorbent. We studied the adsorption capacity (figure 2) as a function of pH of lead and copper using chitosan (CS) and chitosan grafted-poly acrylic acid (CS-*g*-PA) prepared by SI-ATRP.

Adsorption capacities studied at different pH were carried out using l20 mg/L as initial concentration of lead and copper, to ensure no ion precipitation during the experiments. Figure 2 shows two important aspects: first, an increase in the pH of the solution increases the maximum adsorption capacity for both, CS and CS-*g*-PA; however, adsorption capacity is much higher CS-g-PA than for CS. From pH 1 to 2, CS-*g*-PA had a slight greater adsorption, possibly because the chitosan is unstable and tends to solubilize and the acrylate groups are protonated, exhibiting inefficiency to form complexes with ions. However, with the increase of the pH from 3-4, a dramatic increase occurs in the adsorption capacity of copper ions of CS and CS-*g*-PA, from 45.72 to 127.65 and 53.06 mg/g to 147.65 mg/g, while for lead case, an increase from 10.56 to 13.24 and 53.06 to 93.04 occurred. Above of pH 2 becomes apparent that more carboxylate groups are ionized generating an increment in the affinity for cations by electrostatic interactions [24].
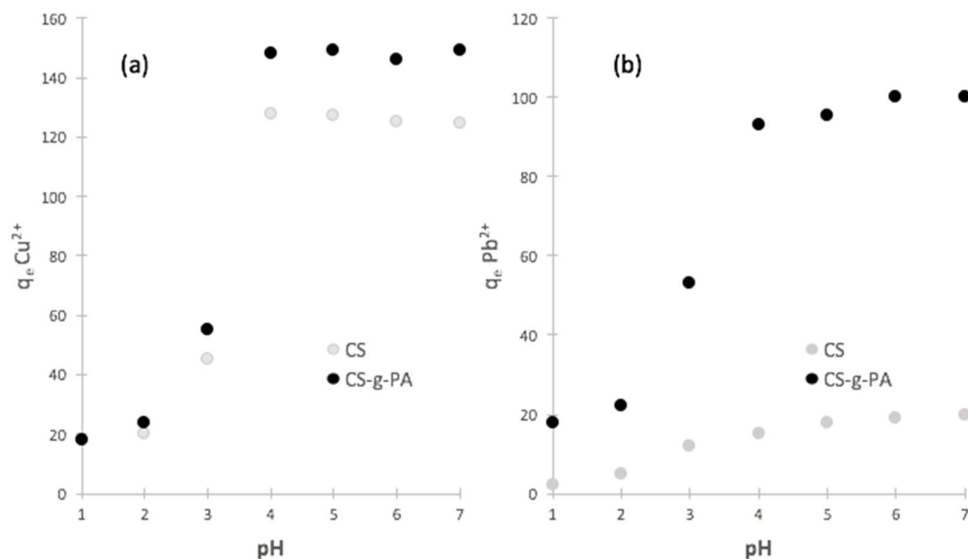
Figure 1. The Effect of pH on the adsorption of (a) Cu2+ and (b) Pb2+ on CS and CS-g-PA. Initial amount of adsorbent: 25 mg, initial volume of samples: 25 mL, at 25°C.

3.2. Adsorption isotherms

Adsorption isotherms describe how the species in solution interact with the adsorbent and also the maximum sorption capacity of the chemical species in solution. Different sorption models are used to fit the experimental data. In this study, Langmuir and Freundlich isotherms were employed to describe the lead and copper adsorption equilibrium. In Langmuir isotherm model, the adsorption process is considered that the adsorbent surface can be covered uniformly with a monolayer of adsorbate. A linear form of the Langmuir equation is:

$$\frac{C_e}{q_e} = \frac{1}{K_L q_m} + \frac{1}{q_m} C_e \qquad (3)$$

Where C_e is the equilibrium concentration of the adsorbate, q the amount of adsorbate per gram; K_L is the Langmuir constant (represents kinetic coefficients of adsorption and desorption); q_m represents the maximum number of ions that can be adsorbed and K_d is related to the adsorption rate. On the other hand, a linear form of the Freundlich equation is:

$$Ln(q) = Ln(k_F) + \frac{1}{n} LnC_{eq} \qquad (4)$$

Where k_F is the Freundlich constant (an indicator of adsorption capacity, the greater the maximum capacity, the greater is k value); furthermore, the ratio $1/n$ is a measure of the intensity of the adsorption [25]. The n and k values are empirical constants and they are specific to the system adsorbent/adsorbate.

Temkin isotherm fit the follow mathematic expression:

$$qe = BlnA + B \ln Ce \qquad (5)$$

where A is the equilibrium binding constant, corresponding to the maximum binding energy and B is the Temkin isotherm constant [25–27].   Figure 3 shows sorption equilibrium of lead and copper ions on CS and CS-*g*-PA surfaces. Fitting results are shown for the three theoretical adsorption models, and table 1 lists fitting parameters for the three models.

Figure 3 shows that the maximum Pb^{2+} adsorption capacity (q_m) increased from q_m=54 mg/g to 81 mg/g after the grafting process. For Cu^{2+}, adsorption capacity (q_m) showed a little improvement from q_m= 133 mg/g to 136 mg/g, after the grafting process. Our results indicate that grafting process improves the maximum capacity for Pb^{2+} and Cu^{2+} ions.   Furthermore, figure 3 and table 1 show that for both metal ions, Langmuir model fit experimental results better the than the Freundlich and Temkin models. These results indicated that the surface of the adsorbent is quite uniform with many equivalent sorption sites, as a product of the grafting process. It is possible that the sorption process occurs through the same mechanism with a monolayer formed through the surface of adsorbate without deposited molecules upon others already adsorbed. For both metal ions, adsorption increased proportionally as concentration increases, suggesting that the active sites of the adsorbent where available for the ions present in the solution, but after a concentration of 200 ppm (for copper) and 300 ppm (for lead), the adsorption value becomes almost constant, because of the saturation of the active sites of the adsorbent. The adsorption on CS-*g*-PA surface in both cases was higher than CS, indicating that acrylate grafting on chitosan surface improved ion adsorption capacity as compare to chitosan without modifications
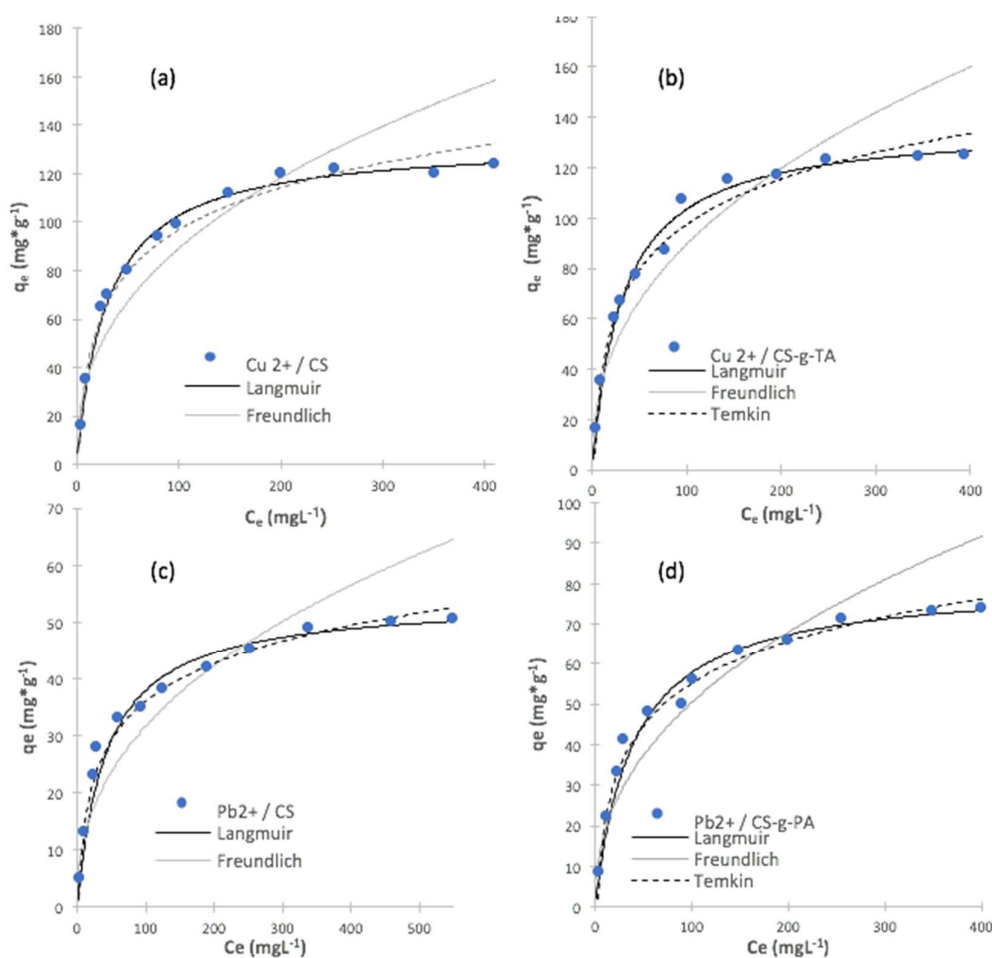

Figure 3. Theoretical model fitting for copper adsorption on (a) CS; (b) CS-g-TA; and theoretical model fitting for lead adsorption on (c) CS and (d) CS-g-TA. (pH: 4.0; adsorption time: 24 hours; initial adsorbent quantity: 25 mg; initial volume: 50 mL; temperature: 25°C).

Table 1. Theoretical Isothermal fitting experimental results.

Isothermal Model	Adsorbent	Metal ion	Parameter (unit)	Value
Langmuir	CS	Cu^{2+}	q_m (mg*g^{-1})	133
			k_L (L*g^{-1})	29.8
			[1]R^2	0.998
		Pb^{2+}	q_m (mg*g^{-1})	54
			K (L*g^{-1})	42.6
			R^2	0.998
	CS-g-TA	Cu^{2+}	q_m (mg*g^{-1})	136
			K (L*g^{-1})	32.3
			R^2	0.998
		Pb^{2+}	Q_m (mg*g^{-1})	80.6
			K (L/g)	39.6
			R^2	0.997
Freundlich	CS	Cu^{2+}	n	2.5
			k	7.1
			R^2	0.867
		Pb^{2+}	n	2.4
			k	4.1
			R^2	0.851
	CS-g-TA	Cu^{2+}	n	2.4
			k	7.0
			R^2	0.891
		Pb^{2+}	n	2.4
			k	5.2
			R^2	0.88
Temkin	CS	Cu^{2+}	A	2.3
			B	25
			R^2	0.978
		Pb^{2+}	A	2.5
			B	9.7
			R^2	0.985
	CS-g-TA	Cu^{2+}	A	2.0
			B	26
			R^2	0.979
		Pb^{2+}	A	2.6
			B	15.2
			R^2	0.990

[1] fitting coefficient.

3.4. Adsorption kinetics for copper and lead ions

The study of adsorption kinetics is important to provide some information about the rate and mechanism of adsorption [28]. Figure 4 shows the variation of the number of adsorbed ions (q_t) as a function of time. The rate of adsorption, for both ions, is high at initial times of adsorption. For both

metals, most of the adsorption takes place within the first 100 minutes, using CS or CS-*g*-PA; however, after this time, we obtained near of 97% of the maximum adsorption. The sorption process is dependent on the sorbent characteristics such as number of functional groups, porosity and number of available sorption sites [29]. The pseudo-second order model is used to study the adsorption data; this model follows equation [30]:

$$\frac{t}{q_t} = \frac{1}{k_2 q_e^2} + \frac{t}{q_e} \qquad (6)$$

where q_t (mg/g) is the adsorption amount at time t (min), k_2 (g/mg*min) is the rate constant of the pseudo-second-order kinetic adsorption. The values of k_2 and q_e are obtained from the intercept and regression coefficient of the experimental t/q_t versus t data; figure 4 shows pseudo-second model fitting and table 2 lists kinetic parameters obtained from the fitting.   Kinetic results revealed that the pseudo-second-order model has suitable agreement with the experimental data. In this model, the rate-limiting step is the surface adsorption that involves chemisorption, where the removal from a solution is due to physicochemical interactions between the two phases [30,31]. Adsorption of Cu^{2+} on CS and CS-g-PA did not show appreciable differences in k_2, however q_e was higher for CS-g-PA than CS. This result suggests that the grafting process increased chitosan surface affinity to Cu^{2+} ion. For Pb^{2+} removal, again q_e was higher for CS-g-PA than CS. In this case, the q_e was 6.6 times higher for CS-g-PA than CS. However, k_2 was 7 times higher for CS than for CS-g-PA; it is well known that the chelation process of cationic ions on aminated surfaces is much lower rate than complexation with carboxylic group-bearing surfaces, which is mainly an electrostatic interaction process; despite k_2 reduces for CS-g-PA adsorbent, final amount of Pb^{2+} removal increased in a factor of 6, which indicates that the process is slower than CS, but CS-g-PA removes 6 times more Pb^{2+}. All these results confirm the importance of the grafting reaction on the chitosan surface for improvement of the maximum uptake and the rate of adsorption process, shaping as a potential useful adsorbent to remove Pb^{2+} and Cu^{2+} ions from wastewaters.
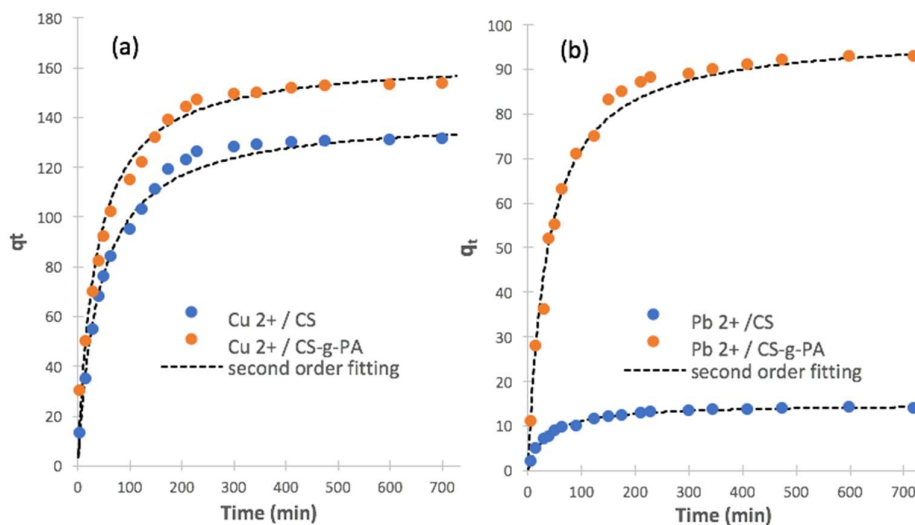

Figure 4. (a) Kinetic adsorption plots for Cu^{2+} on CS and CS-*g*-PA; (b) Kinetic adsorption plots for Pb^{2+} on CS and CS-*g*-PA; inside each plot is shown second linear fitting (initial concentration of Pb (II) and Cu (II) = 20 mg/L; pH = 4; adsorbent = 25 mg; volume of solution = 50 mL; temperature = 25°C.

Table 2. Model kinetic parameters for removal Pb^{2+} and Cu^{2+} by CS and CS-g-PA

adsorbent	Metal Ion	[1]k_2 (g*mg^{-1*}min^{-1}) $^*10^{-4}$	q_e (mg*g^{-1})
	Cu^{2+}	1.7	140
CS	Pb^{2+}	19.8	14.8
	Cu^{2+}	1.8	164
CS-*g*-PA	Pb^{2+}	2.8	98.0

[1] rate constant of the pseudo-second-order kinetic adsorption

4. Conclusions

In this work, we studied the implementation of chitosan grafted-poly acrylic acid as absorbent to remove lead and copper from water. In adsorption kinetic experiments, CS-*g*-PA system had higher adsorption capacity for both metal ions and can be well described by the pseudo-second-order kinetic model according to the *R* values. The maximum uptakes obtained from the kinetic model were close to those from the Langmuir fitting model, except for lead CS adsorption, confirming chemical interactions between adsorbate and adsorbent species. We determined that pH of 4 was the best pH for all the experiments according to the results. For the isotherm experiments, Langmuir model was the best model describing the adsorption equilibrium process according to the linear regression values. The results of this study confirm that chitosan-grafted poly acrylic acid can be used as a potential adsorbent to remove Pb^{2+} and Cu^{2+} ions from wastewaters, with reasonable amounts of adsorbent and consuming short periods of time.

Author Contributions: For research articles with several authors, a short paragraph specifying their individual contributions must be provided. The following statements should be used "Conceptualization, C.G. and F.Z.; Methodology, C.G.; Software, C.G., W.V.; Validation, C.G.; Formal Analysis, C.G., W.V. F.Z.; Investigation, C.G.; Resources, C.G., F.Z.; Data Curation, C.G.; Writing-Original Draft Preparation, C.G., W.V., F.Z.; Writing-Review & Editing, C.G., W.V.; Visualization, C.G., W.V.

Conflicts of Interest:

"The authors declare no conflict of interest.

References

1. Lee, C.-G.; Jeon, J.-W.; Hwang, M.-J.; Ahn, K.-H.; Park, C.; Choi, J.-W.; Lee, S.-H. Lead and copper removal from aqueous solutions using carbon foam derived from phenol resin. *Chemosphere* **2015**, *130*, 59–65, doi:10.1016/J.CHEMOSPHERE.2015.02.055.

2. EPA *Use of Lead Free Pipes, Fittings, Fixtures, Solder and Flux for Drinking Water; Extension of Comment Period*; 2017;

3. Saleh, T. A.; Gupta, V. K. Column with CNT/magnesium oxide composite for lead(II) removal from water. *Environ. Sci. Pollut. Res.* **2012**, *19*, 1224–1228, doi:10.1007/s11356-011-0670-6.

4. Xiao, B.; Thomas, K. M. Competitive Adsorption of Aqueous Metal Ions on an Oxidized Nanoporous Activated Carbon. *Langmuir* **2004**, *20*, 4566–4578, doi:10.1021/LA049712J.

5. Demiral, H.; Güngör, C. Adsorption of copper(II) from aqueous solutions on activated carbon prepared from grape bagasse. *J. Clean. Prod.* **2016**, *124*, 103–113, doi:10.1016/J.JCLEPRO.2016.02.084.

6. WHO publications *Copper in Drinking-water Background document for development of WHO Guidelines for Drinking-water Quality*; Geneva, Switzerland, 2004;

7. Hua, M.; Zhang, S.; Pan, B.; Zhang, W.; Lv, L.; Zhang, Q. Heavy metal removal from water/wastewater by nanosized metal oxides: A review. *J. Hazard. Mater.* **2012**, *211–212*, 317–331, doi:10.1016/J.JHAZMAT.2011.10.016.

8. Karami, H. Heavy metal removal from water by magnetite nanorods. *Chem. Eng. J.* **2013**, *219*, 209–216, doi:10.1016/J.CEJ.2013.01.022.

9. Kumar Gupta, V.; Nayak, A.; Agarwal, S. Bioadsorbents for remediation of heavy metals: Current status and their future prospects. *Environ. Eng. Res* **2015**, *20*, 1–18, doi:10.4491/eer.2015.018.

10. Elieh-Ali-Komi, D.; Hamblin, M. R. Chitin and Chitosan: Production and Application of Versatile Biomedical Nanomaterials HHS Public Access. *Int J Adv Res* **2016**, *4*, 411–427.

11. Zhang, L.; Zeng, Y.; Cheng, Z. Removal of heavy metal ions using chitosan and modified chitosan: A review. *J. Mol. Liq.* **2016**, *214*, 175–191, doi:10.1016/J.MOLLIQ.2015.12.013.

12. Aliabadi, M.; Irani, M.; Ismaeili, J.; Najafzadeh, S. Design and evaluation of chitosan/hydroxyapatite composite nanofiber membrane for the removal of heavy metal ions from aqueous solution. *J. Taiwan Inst. Chem. Eng.* **2014**, *45*, 518–526, doi:10.1016/J.JTICE.2013.04.016.

13. Xu, C.; Wang, J.; Yang, T.; Chen, X.; Liu, X.; Ding, X. Adsorption of uranium by amidoximated chitosan-grafted polyacrylonitrile, using response surface methodology. *Carbohydr. Polym.* **2015**, *121*, 79–85, doi:10.1016/J.CARBPOL.2014.12.024.

14. Zoppe, J. O.; Ataman, N. C.; Mocny, P.; Wang, J.; Moraes, J.; Klok, H.-A. Surface-Initiated Controlled Radical Polymerization: State-of-the-Art, Opportunities, and Challenges in Surface and Interface Engineering with Polymer Brushes. *Chem. Rev.* **2017**, *117*, 1105–1318, doi:10.1021/acs.chemrev.6b00314.

15. Park, D.; Yun, Y.-S.; Cho, H. Y.; Park, J. M. Chromium Biosorption by Thermally Treated Biomass of the Brown Seaweed, *Ecklonia* sp. *Ind. Eng. Chem. Res.* **2004**, *43*, 8226–8232, doi:10.1021/ie049323k.

16. Maria X. Loukidou; Thodoris D. Karapantsios; Anastasios I. Zouboulis, and; Matis*, K. A. Diffusion Kinetic Study of Chromium(VI) Biosorption by Aeromonas caviae. **2004**, doi:10.1021/IE034132N.

17. Sheng, P. X.; Ting, Y.-P.; Chen, J. P.; Hong, L. Sorption of lead, copper, cadmium, zinc, and nickel by marine algal biomass: characterization of biosorptive capacity and investigation of mechanisms. *J. Colloid Interface Sci.* **2004**, *275*, 131–141, doi:10.1016/J.JCIS.2004.01.036.

18. Karthik, R.; Meenakshi, S. Synthesis, characterization and Cr(VI) uptake study of polyaniline coated chitin. *Int. J. Biol. Macromol.* **2015**, *72*, 235–242, doi:10.1016/J.IJBIOMAC.2014.08.022.

19.   Maleki, A.; Pajootan, E.; Hayati, B. Ethyl acrylate grafted chitosan for heavy metal removal from wastewater: Equilibrium, kinetic and thermodynamic studies. *J. Taiwan Inst. Chem. Eng.* **2015**, *51*, 127–134, doi:10.1016/J.JTICE.2015.01.004.

20.   Li, N.; Renbi Bai, A.; Liu, C. Enhanced and Selective Adsorption of Mercury Ions on Chitosan Beads Grafted with Polyacrylamide via Surface-Initiated Atom Transfer Radical Polymerization. *Langmuir* **2005**, *21*, 11780–11787, doi:10.1021/LA051551B.

21.   Grande, C. D.; Alí, F.; Zuluaga, F. Síntesis de quitosano modificado con poli (ácido acrílico) vía polimerización por transferencia atómica iniciada desde la superficie(SIP-ATRP). *Iberoam. Polím* **2010**, *11*, 505–514.

22.   Moad, G.; Rizzardo, E.; Solomon, D. H. Selectivity of the reaction of free radicals with styrene. *Macromolecules* **1982**, *15*, 909–914, doi:10.1021/ma00231a042.

23.   Ng, J. C. Y.; Cheung, W. H.; McKay, G. Equilibrium studies for the sorption of lead from effluents using chitosan. *Chemosphere* **2003**, *52*, 1021–1030, doi:10.1016/S0045-6535(03)00223-6.

24.   Wang, X.; Kim, Y.-G.; Drew, C.; Ku, B.-C.; Kumar, J.; Samuelson, L. A. Electrostatic Assembly of Conjugated Polymer Thin Layers on Electrospun Nanofibrous Membranes for Biosensors. *Nanoletters* **2004**, *4*, 331–334, doi:10.1021/NL034885Z.

25.   James E. House *Principles of Chemical Kinetics*; second.; Academic Press: Suite 400, Burlington, MA 01803, USA, 2007; ISBN 978-0-12-356787-1.

26.   Saha, P.; Chowdhury, S.; Gupta, S.; Kumar, I. Insight into adsorption equilibrium, kinetics and thermodynamics of Malachite Green onto clayey soil of Indian origin. *Chem. Eng. J.* **2010**, *165*, 874–882, doi:10.1016/J.CEJ.2010.10.048.

27.   Inyinbor, A. A.; Adekola, F. A.; Olatunji, G. A. Kinetics, isotherms and thermodynamic modeling of liquid phase adsorption of Rhodamine B dye onto Raphia hookerie fruit epicarp. *Water Resour. Ind.* **2016**, *15*, 14–27, doi:10.1016/j.wri.2016.06.001.

28.   Aljeboree, A. M.; Alshirifi, A. N.; Alkaim, A. F. Kinetics and equilibrium study for the adsorption of textile dyes on coconut shell activated carbon. *Arab. J. Chem.* **2017**, *10*, S3381–S3393, doi:10.1016/J.ARABJC.2014.01.020.

29.   Annadurai, G.; Juang, R. S.; Lee, D. J. Adsorption of heavy metals from water using banana and orange peels. *Water Sci. Technol.* **2003**, *47*.

30.   Robati, D. Pseudo-second-order kinetic equations for modeling adsorption systems for removal of lead ions using multi-walled carbon nanotube. *J. Nanostructure Chem.* **2013**, *3*, 55, doi:10.1186/2193-8865-3-55.

31.   Wang, H.; Zhou, A.; Peng, F.; Yu, H.; Yang, J. Mechanism study on adsorption of acidified multiwalled carbon nanotubes to Pb(II). *J. Colloid Interface Sci.* **2007**, *316*, 277–283, doi:10.1016/j.jcis.2007.07.075.